Chinese Chemical Letters 34 (2023) 107504

Contents lists available at ScienceDirect

Chinese Chemical Letters

journal homepage: www.elsevier.com/locate/cclet

A new strategy to design isostructural salts: The case of the antitumor drug dimethylaminomicheliolide

Zhonghua Li[a], Haibin Qu[a], Lan Fang[a], Songgu Wu[a,*], Junbo Gong[a,b,*]

[a] State Key Laboratory of Chemical Engineering, School of Chemical Engineering and Technology, Tianjin University, Tianjin 300072, China
[b] Chemistry and Chemical Engineering Guangdong Laboratory, Shantou 515031, China

ARTICLE INFO

Article history:
Received 12 April 2022
Revised 27 April 2022
Accepted 10 May 2022
Available online 13 May 2022

Keywords:
Dimethylaminomicheliolide
Crystal engineering
Isostructural salt
Intermolecular interactions
Thermal analysis
Hygroscopicity
Solubility

ABSTRACT

Isostructural multicomponent crystals provide a promising way for fine-tuning physicochemical properties, whereas their design remains quite challenging. The purpose of this work was to provide a new strategy for obtaining isostructural multicomponent crystals by introducing coformers with functional group positional isomerism. Five isostructural salts of an antitumor drug dimethylaminomicheliolide (DMAMCL) were reported and designed with a series of dihydroxybenzoic acid regioisomers for the first time, which were identified by power and single-crystal X-ray diffractions. Similar lattice parameters suggested these obtained salts may have the same crystal packing mode. The quantitative similarity parameters *via* XPac, CrystalCMP and Mercury program further proved these crystal structures are 3D isostructural. Hirshfeld surface maps and 2D fingerprint plots show that the isostructural salts have similar intermolecular interactions. Compared with DMAMCL, obvious improvement was observed in the thermal stability, hygroscopicity, and solubility of these isostructural salts. Meanwhile, isostructural crystals may have different physicochemical properties, even though the shape and molecular size are similar and the packing of crystal structures is equally matched.

Solid state forms exploration has always been an important subject in the field of crystal engineering, and it plays a major role in the development of pharmaceuticals, food additives, organic pigments and energetic materials [1–4]. A number of solid-state properties, such as solubility [5], dissolution rate [6], mechanical performance [7,8], and optical and electrical properties [9,10] of organic molecules are critically dependent on their crystal structures including molecular conformations and crystal packing modes. The core mission of solid-state chemistry research is to regulate molecular assembly to achieve the best performance in specific applications [11].

Isostructural multicomponent crystals have more obvious advantages than polymorphs in adjusting molecular packing, and have received great attention [12,13]. For example, isostructural crystals can be used as special templates or additives to discover new crystal forms [14], prepare single crystals [15], realize the controllable preparation of metastable polymorphs [16] or design solid solutions [17]. However, the design and synthesis of isostructural crystals is still full of challenges. Organic molecules possess various sizes, intricate shapes and complex weak intermolecular interactions. Thus, slight changes in molecular structure may affect the assembly mode. Most of the current studies on isostructural crystals mainly focus on the report of isostructural solvates [18–22], while the isostructurality of cocrystals or salts is a comparatively rare phenomenon [23]. Moreover, previous studies mainly selected a series of coformers with equivalent atomic substitution such as O/S [24], Br/I [11], Cl/CH_3 [25], and there is no uniform and applicable empirical rule for designing isostructural multicomponent crystals. Therefore, it is necessary to carry out detailed studies to explore other possible design strategies of isostructural crystals to accumulate more knowledge or expand corresponding applications.

Here, we report dimethylaminomicheliolide (DMAMCL) as a case to design isostructural salts by exploiting a series of dihydroxybenzoic acid regioisomers [2,3-dihydroxybenzoic acid (23DBA); 2,4-dihydroxybenzoic acid (24DBA); 2,5-dihydroxybenzoic acid (25DBA); 3,4-dihydroxybenzoic acid (34DBA) and 3,5-dihydroxybenzoic acid (35DBA) molecules, Fig. 1]. DMAMCL demonstrates outstanding antitumor effects, while poor water solubility limits its clinical application [26]. The relatively rigid molecular skeleton supports a good structural foundation for the design of isostructural crystals. All five obtained DMAMCL-based salts were fully characterized with power and single-crystal X-ray

* Corresponding authors.
E-mail addresses: wusonggu@tju.edu.cn (S. Wu), junbo_gong@tju.edu.cn (J. Gong).

https://doi.org/10.1016/j.cclet.2022.05.018
1001-8417/

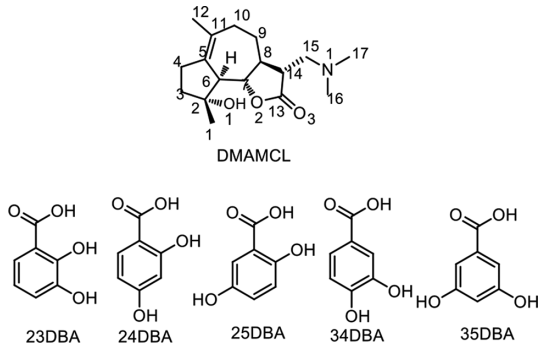

Fig. 1. Chemical structures of DMAMCL and coformers.

diffractions (PXRD and SCXRD), thermogravimetric analysis (TGA), differential scanning calorimetry (DSC), and polarizing microscopy (PLM). Dynamic vapor sorption (DVS) experiments and equilibrium solubility measurement were conducted to improve the corresponding physicochemical properties of DMAMCL. Fingerprint plots and the quantitative similarity parameters calculated from various programs showed that these DMAMCL-based salts are 3D isostructural.

Powder samples of the DMAMCL-based salts were prepared with the slurry method, and the corresponding single crystals were successfully obtained by slow evaporation or cooling of saturated solution experiments in ethyl acetate, acetonitrile or acetone for the first time. The detailed preparation procedures are presented in Table S1 (Supporting information). The PXRD patterns (Fig. S1 in Supporting information) of newly discovered phases present obvious differences compared with their parent compounds (Fig. S2 in Supporting information), and the simulated PXRD patterns (Fig. S3 in Supporting information) were closely matched with the experimental patterns obtained from the relevant powder samples, which confirms the formation of highly pure phases. PXRD data showed many similar powder diffraction peaks among the new phases, suggesting that these five DMAMCL-based multicomponent crystals may have some similarities in the crystal packing mode or belong to isostructural crystals. PLM pictures (Fig. S4 in Supporting information) show that the morphology of these isostructural crystals is not exactly the same. This is not difficult to understand, and the crystal morphology is not only affected by its own crystal structure, but also regulated by a variety of external crystallization conditions [27,28].

Five multicomponent crystals (DMAMCL-23DBA, DMAMCL-24DBA, DMAMCL-25DBA, DMAMCL-34DBA and DMAMCL-35DBA) exhibit similar lattice parameters (Table S2 in Supporting information). They all crystallize in an orthorhombic crystal system with the same space group $P2_12_12_1$. The thermal ellipsoid drawings show that one DMAMCL cation and one corresponding acid anion are contained in their asymmetric units for these five DMAMCL salts (Figs. S5-S9 in Supporting information). Similar lattice parameters may represent similar crystal packing and molecular assembly modes, which are usually affected by the conformation of the host molecule. The conformation superposition result shows that they are almost indistinguishable (Fig. 2), and the maximum difference for the observed torsion angle τ (C9-C8-C14-C15) is only about 10° (Table 1). Such subtle conformational differences imply that the intermolecular interactions formed in these salts will better follow the synthons.

The hydrogen bond data containing bond lengths and valence angles are summarized in Table S3 (Supporting information), which shows that the main hydrogen bond interactions in these DMAMCL-based salts were similar. An intramolecular hydrogen bond O1–H1···O2 formed between an ester moiety and hydroxyl

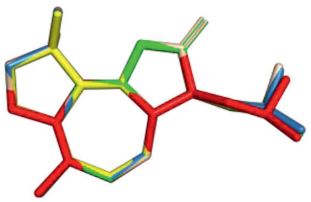

Fig. 2. Overlays of DMAMCL molecular conformations (red, DMAMCL-23DBA; green, DMAMCL-24DBA; yellow, DMAMCL-25DBA; wheat, DMAMCL-34DBA; sky-blue, DMAMCL-35DBA).

Table 1
Torsion angles (τ, °) in various conformers of DMAMCL.

Salt	τ 1	τ 2	τ 3	τ 4
DMAMCL-23DBA	−89.16	148.28	−160.97	74.40
DMAMCL-24DBA	−78.95	158.07	−165.87	70.52
DMAMCL-25DBA	−80.83	155.38	−165.39	71.45
DMAMCL-34DBA	−79.04	157.68	−166.15	70.48
DMAMCL-35DBA	−84.63	152.53	−164.85	70.88

τ 1: τ (C9-C8-C14-C15); τ 2: τ (C7-C8-C14-C15); τ 3: τ (C17-N1-C15-C14); τ 4: τ (C16-N1-C15-C14).

group appeared in the DMAMCL molecule. The adjacent dihydroxybenzoic acid molecules form a 1D chain through an intermolecular O7–H7A···O5 and/or O6–H6A···O5 typical hydrogen bonds or weak C–H···O hydrogen bonds along the *b*-axis (Fig. S10 in Supporting information). Meanwhile, a common O–H···O intramolecular hydrogen bond between the carboxylic acid group and ortho hydroxyl group was involved in 23DBA, 24DBA and 25DBA molecules. Dihydroxybenzoic acid molecules act as a bridge connecting DMAMCL molecules *via* N–H···O and O–H···O hydrogen bonds, and then the host molecular tape and conformer molecular tape are alternately arranged along the *a*-axis. Weak hydrogen bonds including C–H···O and C–H···π, π···π contacts and van der Waals interactions mainly play an important role in the construction of 3D packing structures (Fig. 3), and the coformer molecules seem to be filled in the cavity holes surrounded by the DMAMCL molecules in the *ac* plane. When the corresponding coformers are removed from the 3D structures of the DMAMCL salts, the remaining voids (coformer occupied spaces) are presented as a golden cloud in Fig. S11 (Supporting information). The order of space occupied by coformers is 25DBA (639.99 Å^3) > 24DBA (626.67 Å^3) > 34DBA (614.70 Å^3) > 23DBA (609.91 Å^3) > 35DBA (597.78 Å^3). Although the five selected dihydroxybenzoic acid coformers belong to positional isomers, they still have similar potential complementary functional groups to form synthons with host molecules, which is beneficial to the formation of isostructural multicomponent crystals and brings precise regulation of physicochemical properties.

The values of the unit cell similarity index (π) [29] and mean elongation (ε) [30] were calculated and found to be close to zero (Table S4 in Supporting information), which further supports the isostructurality. DMAMCL-24DBA and DMAMCL-25DBA have the highest similarity on the basis of the smallest values of π and ε. We speculate that this is mainly because the molecular volumes and shapes of 24DBA and 25DBA are the closest. Furthermore, the relatively low values of PS_{ab} (0.2∼1.6, Fig. S12 in Supporting information) obtained from CrystalCMP software show that the packing of DMAMCL is similar in all the obtained salts, which is consistent with the crystal structure analysis. Based on the similarity of geometric parameters of different structures, the Xpac program was used to identify and compare the possible molecule packing similarity in 0D/1D/2D/3D dimensions [31]. The XPac dissimilarity index value is between 2.0∼10.5 (Fig. 4). Such small values are indicative of 3D isostructurality between each pair of crystal structures of the corresponding DMAMCL salts. Comparatively speak-

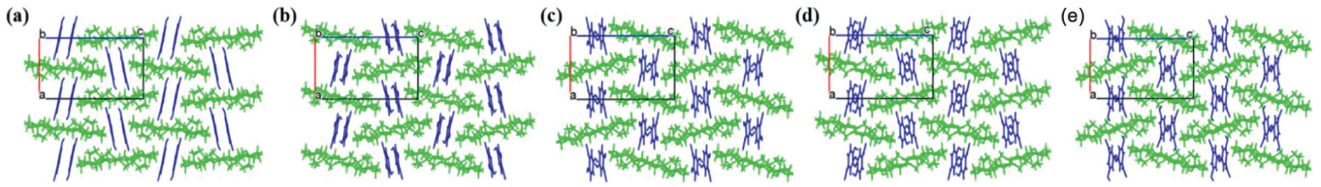

Fig. 3. Packing view of (a) DMAMCL-23DBA, (b) DMAMCL-24DBA, (c) DMAMCL-25DBA, (d) DMAMCL-34DBA and (e) DMAMCL-35DBA in the *ac* plane.

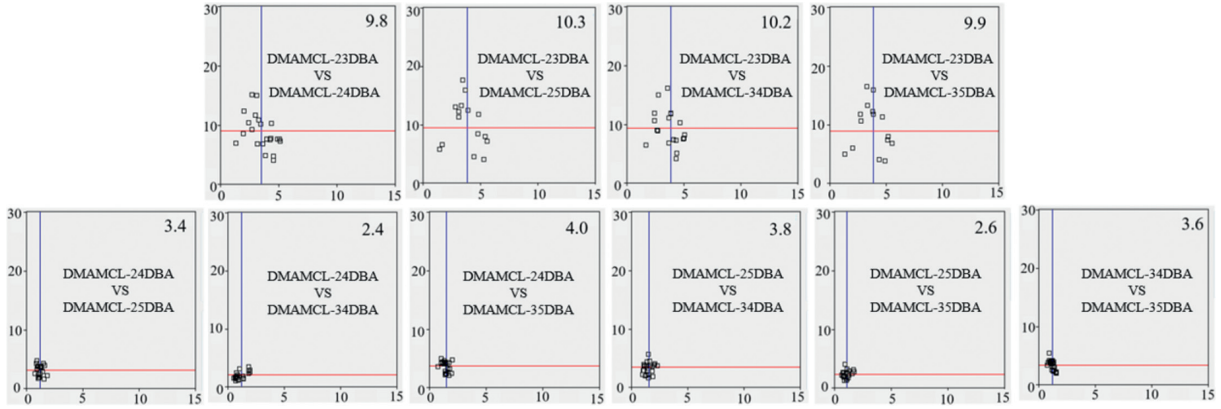

Fig. 4. Plots of interplanar angular deviation *vs.* angular deviation in XPac with various dissimilarity index values for five DMAMCL salts.

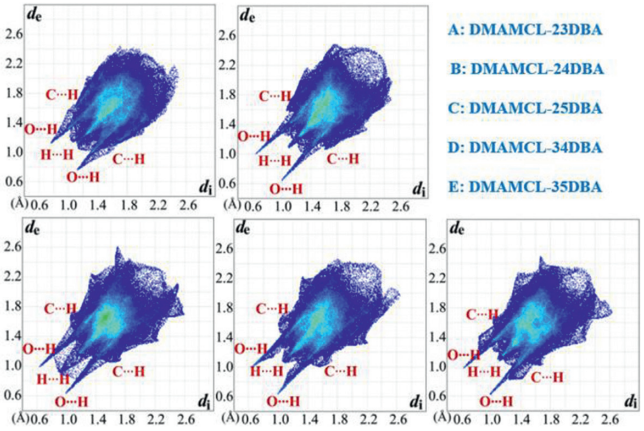

Fig. 5. 2D fingerprint plots of isostructural salts.

ing, the dissimilarity index values are larger for four pairs (9.8 for DMAMCL-23DBA and DMAMCL-24DBA; 10.3 for DMAMCL-23DBA and DMAMCL-25DBA; 10.2 for DMAMCL-23DBA and DMAMCL-34DBA; 9.9 for DMAMCL-23DBA and DMAMCL-35DBA), which indicates that they have smaller packing similarity. This is mainly due to steric hindrance of 23DBA, and the difference in the position of functional groups will further lead to a change in their roles in the assembly of multicomponent crystal molecules. In addition, the calculated PXRD similarity index values are between 0.97 and 0.99 (Table S5 in Supporting information) suggesting that the five DMAMCL salts are 3D isostructural, which is consistent with the conclusions obtained by other similarity analysis methods.

Hirshfeld surface was used to characterize and quantify the intermolecular interactions of these salts [32]. The obvious red spots on the surface (Fig. S13 in Supporting information) indicated the presence of N–H···O or O–H···O contacts and facilitated the formation of heterodimer synthons. 2D fingerprint plots show that the five isostructural salts discussed above have common characteristics (Fig. 5). Strong O···H interactions appeared as forceps-like spikes, which contributed 28.3%–31.6% of the total interactions. The weakest H···H contacts spread over a large area, which contributed a major contribution of 54.6%–57.7% of the total interaction to the Hirshfeld surface. Moreover, three quantitative parameters of Hirshfeld surfaces containing molecular volume, Hirshfeld surface area and globularity of the surface were similar respectively (Fig. S14 in Supporting information).

All the obtained DMAMCL-based salts were characterized by TGA and DSC (Figs. S15 and S16 in Supporting information). Each of the isostructural salts was found to exhibit a melting point between the melting points of both ingredients. The melting point of DMAMCL-24DBA is approximately 26 °C higher than that of DMAMCL-23DBA. The order of the melting point for these isostructural salts seems not to be consistent with that of the coformers (35DBA > 24DBA > 23DBA > 25DBA > 34DBA) or the order of lattice energy [DMAMCL-34DBA (−183.75 kcal/mol) > DMAMCL-35DBA (−177.28 kcal/mol) > DMAMCL-24DBA (−165.48 kcal/mol) > DMAMCL-25DBA (−165.17 kcal/mol) > DMAMCL-23DBA (−163.25 kcal/mol)].

Sometimes the melting point is also affected by crystal packing in addition to intermolecular interactions, and the crystal density can reflect the packing tightness of crystals to some extent. Generally, the higher the crystal density, the closer the crystal packing, and the higher the melting point of crystals. The molecular volume ordering does show the opposite trend with the crystal density ordering [DMAMCL-23DBA (1.296 g/cm^3) < DMAMCL-24DBA (1.299 g/cm^3) < DMAMCL-25DBA (1.306 g/cm^3) < DMAMCL-34DBA (1.318 g/cm^3) < DMAMCL-35DBA (1.355 g/cm^3)]. However, these two physical parameters still cannot match the melting point ordering well. Therefore, the melting point of these isostructural salts cannot be simply related to a certain variable, but is more likely to be influenced by many factors such as the physicochemical properties of coformers, intermolecular interactions and compactness of crystal packing. Moreover, the influence of relative humidity on these isostructural salts was investigated with DVS measurements at 25 °C. As shown in the vapor sorption isotherms (Fig. S17 in Supporting information), DMAMCL-24DBA, DMAMCL-25DBA and DMAMCL-34DBA salts absorbed 0.33%, 1.10% and 0.41% moisture at 95% RH, respectively. In contrast, the DMAMCL-23DBA and

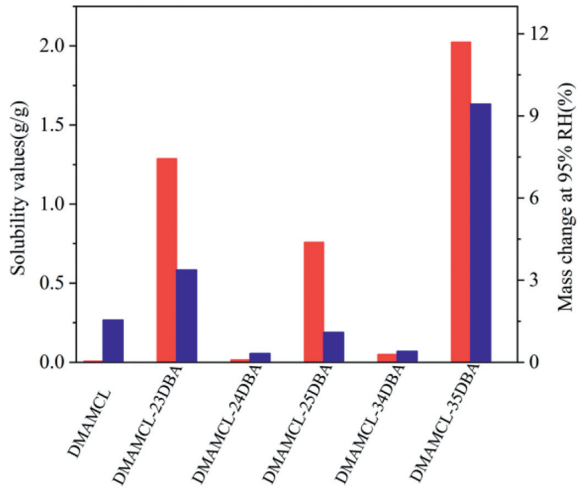

Fig. 6. Solubility profile and mass change at 95% RH of DMAMCL and its isostructural salts.

DMAMCL-35DBA salts exhibit totally different sorption behaviors. From 0% to 95% RH, DMAMCL-23DBA salt absorbed 3.38% moisture. DMAMCL-35DBA salt absorbed about only 1.77% at 75% RH, while it remarkably absorbed moisture above 75% RH and absorbed 9.44% of water at 95% RH. In order to further determine whether the phase transformation behavior occurs after water adsorption or desorption for the isostructural salts, we conducted PXRD analysis on the samples before and after the DVS tests. The PXRD patterns (Fig. S18 in Supporting information) show that the positions of the characteristic diffraction peaks of these isostructural salts after adsorption/desorption are consistent with the corresponding initial samples. Meanwhile, no dehydration endothermic peaks appeared in the DSC curves (Fig. S19 in Supporting information) of the samples after adsorption. These results indicate that no phase transformation happens for the isostructural salts, and the adsorbed water only exists in the form of physical adsorption. Furthermore, Fig. 6 shows that the solubility of DMAMCL (pH 6.8, 37 °C) can in fact be improved by a factor of 2–275 without altering the molecular structure of DMAMCL.

In conclusion, five isostructural organic salts of DMAMCL were first obtained with the help of dihydroxybenzoic acid positional isomers. The successful synthesis of isostructural crystals is mainly attributed to the robust synthons between DMAMCL molecule and dihydroxybenzoic acid molecule, the extremely small difference of molecular conformations and the high similarity of coformer size and shape. The isostructurality of series of salts were confirmed with the analysis of Hirshfeld surface maps, 2D fingerprint plots and quantitative similarity parameters from XPac, CrystalCMP, and Mercury software. Our research also shows that the thermal behaviors, hygroscopicity and solubility of isostructural crystals could be different although the packing of structure is equally matched. More importantly, this work provides a successful case of designing isostructural multicomponent crystals and we hope that it will bring some inspiration for the design and application development of higher order organic crystals.

Declaration of competing interest

The authors report no declarations of interest.

Acknowledgments

This work was financially supported by the Key R&D Project of Hebei Province (No. 21282602Z) and Shandong Province (No. 2020CXGC010506) and the Innovative Group Project (No. 21621004).

Supplementary materials

Supplementary material associated with this article can be found, in the online version, at doi:10.1016/j.cclet.2022.05.018.

References

[1] J. Aaltonen, M. Allesø, S. Mirza, et al., Eur. J. Pharm. Biopharm. 71 (2009) 23–37.
[2] B. Zhou, D. Yan, Appl. Phys. Rev. 8 (2021) 041310.
[3] D. Yan, Chem. Eur. J. 21 (2015) 4880–4896.
[4] Y. Lu, Y. Tang, H. Lin, et al., Chin. Chem. Lett. 29 (2018) 1541–1543.
[5] P. Sanphui, S.S. Kumar, A. Nangia, Cryst. Growth Des. 12 (2012) 4588–4599.
[6] D. Yang, H. Wang, Q. Liu, et al., Chin. Chem. Lett. 33 (2022) 3207–3211.
[7] K. Zhang, C.C. Sun, Y. Liu, et al., Chem. Mater. 33 (2021) 1053–1060.
[8] S. Dey, S. Das, S. Bhunia, et al., Nat. Commun. 10 (2019) 3711.
[9] H. Wu, Y. Sun, L. Sun, et al., Chin. Chem. Lett. 32 (2021) 3007–3010.
[10] Y. Chen, Z. Chang, J. Zhang, et al., Angew. Chem. 133 (2021) 22598–22605.
[11] B. Lu, S. Liu, D. Yan, Chin. Chem. Lett. 30 (2019) 1908–1922.
[12] D. Cinčić, T. Friščić, W. Jones, New J. Chem. 32 (2008) 1776–1781.
[13] S. Li, B. Lu, X. Fang, et al., Angew. Chem. Int. Ed. 59 (2020) 22623–22630.
[14] A. Levesque, T. Maris, J.D. Wuest, J. Am. Chem. Soc. (2020) 11873–11883.
[15] V.K. Srirambhatla, R. Guo, S.L. Price, et al., Chem. Commun. 52 (2016) 7384–7386.
[16] R. Telford, C.C. Seaton, A. Clout, et al., Chem. Commun. 52 (2016) 12028–12031.
[17] M.K. Mishra, U. Ramamurty, G.R. Desiraju, J. Am. Chem. Soc. 137 (2015) 1794–1797.
[18] K.B. Landenberger, O. Bolton, A.J. Matzger, Angew. Chem. 125 (2013) 6596–6599.
[19] J. Wojnarska, M. Gryl, T. Seidler, et al., Cryst. Growth Des. 20 (2020) 6535–6544.
[20] O. Dwichandra Putra, E. Yonemochi, H. Uekusa, Cryst. Growth Des. 16 (2016) 6568–6573.
[21] H.D. Clarke, M.B. Hickey, B. Moulton, et al., Cryst. Growth Des. 12 (2012) 4194–4201.
[22] J. Galcera, T. Friščić, E. Molins, et al., CrystEngComm 15 (2013) 1332–1338.
[23] J. Wojnarska, M. Gryl, T. Seidler, et al., Cryst. Growth Des. 20 (2020) 6535–6544.
[24] D. Cinčić, T. Friščić, W. Jones, Chem. Eur. J. 14 (2008) 747–753.
[25] S.K. Nechipadappu, D.R. Trivedi, J. Mol. Struct. 1141 (2017) 64–74.
[26] Q. Zhang, Y. Lu, Y. Ding, et al., J. Med. Chem. 55 (2012) 8757–8769.
[27] D. Han, T. Karmakar, Z. Bjelobrk, et al., Chem. Eng. Sci. 204 (2019) 320–328.
[28] Z.H. Li, P. Shi, Y. Yang, et al., CrystEngComm 21 (2019) 3731–3739.
[29] A. Kálmán, G. Argay, et al., Acta Crystallogr. Sect. B: Struct. Sci. 47 (1991) 68–77.
[30] L. Fábián, A. Kálmán, Acta Crystallogr. Sect. B: Struct. Sci. 55 (1999) 1099–1108.
[31] T. Gelbrich, T.L. Threlfall, M.B. Hursthouse, CrystEngComm 14 (2012) 5454–5464.
[32] J.J. Mckinnon, D. Jayatilaka, M.A. Spackman, Chem. Commun. (2007) 3814–3816.